Oxidation of sputtered AlScN films exposed to the atmosphere

Minghua Li
Institute of Microelectronics
*Agency for Science, Technology and Research (A*STAR)*
Singapore
li_minghua@ime.a-star.edu.sg

Kan Hu
Institute of Microelectronics
*Agency for Science, Technology and Research (A*STAR)*
Singapore
hu_kan@ime.a-star.edu.sg

Huamao Lin
Institute of Microelectronics
*Agency for Science, Technology and Research (A*STAR)*
Singapore
lin_huamao@ime.a-star.edu.sg

Valery Felmetsger
(Visiting Scientist)
Institute of Microelectronics
*Agency for Science, Technology and Research (A*STAR)*
Singapore
felmetsger@yahoo.com

Yao Zhu
Institute of Microelectronics
*Agency for Science, Technology and Research (A*STAR)*
Singapore
zhuya@ime.a-star.edu.sg

***Abstract*—1 µm thick highly *c*-axis textured $Al_{0.8}Sc_{0.2}N$ films were fabricated using Pulsed DC reactive magnetron sputtering. The as-deposited films were exposed to the atmosphere for about one month before characterization. X-ray photoelectron spectroscopy (XPS) and Transmission Electron Microscopy (TEM) revealed the formation of an oxide overlayer on AlScN film surface, which directly contacted to air. Reaction controlled process was responsible for this self-limited oxidation. In AlScN film with small grains and big portion of grain boundary, oxygen was also detected at the grain boundaries in bulk film. The oxidation reaction modulates AlScN film composition and surface structure, which would pose additional challenges for the AlScN-based device design and integration.**

Keywords—scandium aluminum nitride, chemical stability, surface oxidation, oxygen diffusion along grain boundary

I. Introduction

Scandium doped aluminum nitride (AlScN) thin films inspire a wide variety of novel device development, owning to their good piezoelectric response, large remnant polarization, and CMOS compatible integration capability [1-3]. Reliability of these devices highly depends on material stability. Air-exposed aluminum nitride (AlN) can be partially oxidized, resulting in property change and film quality degradation. It has been reported [4] that oxidation of AlN film caused increase in insertion loss in the AlN-based SAW devices. Another work demonstrated that surface oxidation of AlN film led to decrease of piezoelectric constant [5].

Surface oxidation has been observed on AlScN films, too. A ~ 4 nm oxide layer was found on $Al_{0.58}Sc_{0.32}N$ and $Al_{0.54}Sc_{0.36}N$ films deposited using reactive co-sputtering [6, 7]. The oxide overlayer was generated during prolonged exposure of the as-deposited AlScN film to air. Using Transmission Electron Microscopy (TEM), oxygen was found on the film surface but not in the bulk AlScN. Therefore the electronic device functioned well [8]. However, the oxidation reaction mechanism and its effect on the device performance have not been discussed.

In this work, we fabricated $Al_{0.8}Sc_{0.2}N$ film on molybdenum (Mo) substrate, and stored it in clean room environment. Crystallographic texture and chemical composition distribution of the AlScN film were characterized. Oxidation reaction mechanism was also discussed.

II. Experimental

A. Sputtering of AlScN film

We utilized a multi-chamber sputtering system to prepare samples. On a 200 mm Si substrate, 20 nm AlN and 100 nm Mo film were firstly made. Without vacuum break, the wafer was transferred to another chamber for 1 µm AlScN film deposition. This sputtering chamber was equipped with a pulsed-DC magnetron source and an $Al_{80}Sc_{20}$ alloy target [9]. Reactive gas N_2 and discharge gas Ar were introduced into the chamber for reactive sputtering. No substrate heating was applied during the AlScN film deposition.

B. Exposure to the atmosphere

The as-deposited AlScN/Mo film stacks were kept in the high vacuum sputtering system until the wafers cooled down to room temperature before unloading. The samples were stored in a semiconductor clean room environment for one month. Temperature and relative humidity were ~21 °C and 30 – 50 %, respectively.

C. Characterization methods

Film orientation and texture were inspected by high-resolution X-ray Diffraction (XRD) technology. Surface morphology and chemical composition were evaluated using a Transmission Electron Microscopy (TEM) coupled with Energy-dispersive X-ray Spectroscopy (EDX). The cross-sectional TEM lamellae were prepared by a Focused Ion Beam

(FIB) tool. Elemental distribution was characterized using X-ray Photoelectron Spectroscopy (XPS) depth profiling. All characterization experiments were conducted at room temperature.

III. Results and Discussion

Fig. 1a displays the XRD ω - 2θ pattern recorded in 2θ range from 20° to 80°. Apart from the Si (100) peak caused by the substrate, only Wurtzite AlScN {0001} and body-centered cubic Mo (110) reflection peaks were detected. The peaks at 2θ of 35.98° and 76.10° were assigned to AlScN (0002) and AlScN (0004) reflections, respectively. In addition, the peak located at 2θ = 40.50° was assigned to Mo (110). The XRD rocking curve of the AlScN (0002) reflection was also measured and shown in Fig. 1b. The Full-Width-at-Half-Maximum (FWHM) value was 1.3°, demonstrating good *c*-axis texture of the AlScN film.

Cross-sectional TEM image in Fig. 2a shows the columnar textured AlScN film. The diameter of the columnar grains ranges from 30 to 50 nm, which is comparable to our previous data on $Al_{0.85}Sc_{0.15}N$ film [10]. Due to remarkable image contrast difference, a thin layer was noticed on the AlScN film surface. This overlayer became more clearly seen on the high-resolution TEM image (Fig. 2b). The thickness was 10 – 20 nm. In Ref [8], similar overlayer on AlScN film surface was identified as oxide using EDX elemental map.

Because of high depth resolution and precise composition analysis capabilities [11], we used XPS depth profiling to characterize the chemical composition and the elemental distribution through the AlScN film thickness. A low power Ar^+ gun was used to gradually sputter off the film step- by-step from surface. After each sputtering step, XPS core-level spectra were scanned on N 1s, O 1s, Al 2p, and Sc 2p and then their atomic percentages were determined. Fig. 3 shows the XPS depth profile, which reflects the elemental distribution along the film thickness direction. Significantly high oxygen and low nitrogen concentrations were found at the film surface, which corresponds to the sputtering time of zero. As the measurement spot moved towards the substrate, the oxygen concentration decreased rapidly, and became negligible in the bulk film region. Meanwhile, the film composition recovered to stoichiometric $Al_{0.8}Sc_{0.2}N$. It demonstrated that surface oxidation happens on the AlScN film. It is a self-limited process and agrees to the reactive-controlled surface oxidation mechanism on AlN films [12, 13]. Only the film surface with direct contact with air was oxidized.

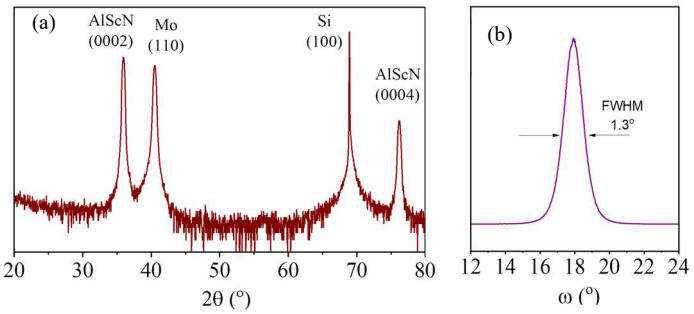

Fig. 1. XRD patterns of the ScAlN/Mo film stack: (a) ω - 2θ scan, and (b) rocking curve of AlScN (0002) reflection. The FWHM value 1.3° demonstrated good *c*-axis AlScN film texture.

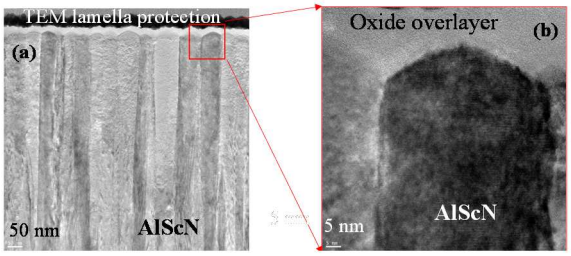

Fig. 2. TEM (a) and high-resolution TEM (b) images near the AlScN top surface. The obvious image contrast on the film surface suggests additional material generation when exposed to the atmosphere.

When the AlScN film had small grains and big portion of grain boundaries [14, 15], oxidation in bulk film was found. Fig. 4 displays the scanning TEM image coupled with the EDX line analysis results. The EDX analysis line was set parallel to the substrate and located more than 100 nm away from the film surface. Oxygen was detected at grain boundaries. Conversely, nitrogen, aluminium, and scandium amounts decreased at the same locations. It is well known that mass density of the grain boundaries is lower [16], which gives rise of percolation paths for oxygen to propagate into the bulk AlScN film.

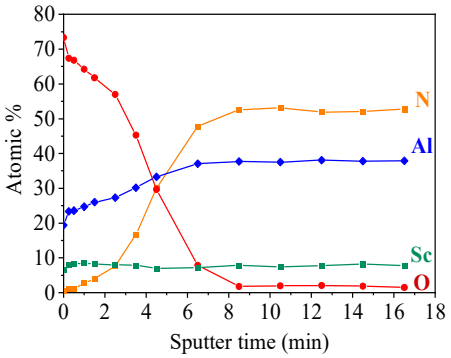

Fig. 3 XPS depth profile showing the elemental distribution from film surface (Sputter time equals to zero) to the substrate. High concentration of oxygen at the film surface indicates the surface oxidation.

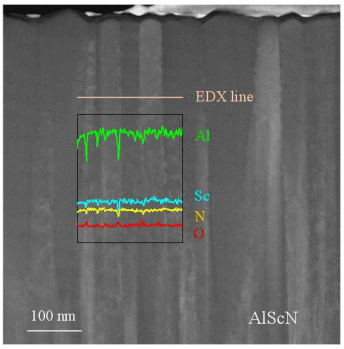

Fig. 4 Scanning TEM image and EDX line analysis in the AlScN bulk film. The analysis line was set more than 100 nm away from the film surface. High oxygen was found at grain boundaries, which acted as percolation paths for oxygen to diffuse into the film.

IV. CONCLUSIONS

When the as-sputtered AlScN film exposed to the atmosphere, oxygen reacts with the AlScN and generates an oxide overlayer with thickness of 10-20 nm. The surface oxidation is self-limited and reaction controlled. In the film with small grains and big portion of grain boundaries, oxygen was also found at grain boundaries in the bulk film. We believe that the low-density grain boundaries function as percolation paths for oxygen to diffuse into the bulk film.

Oxidation of AlScN modifies the film surface composition and microstructure. As the AlScN film thickness scaling down, surface contributes more pronouncedly to the overall film performance. AlScN film stability should be well addressed during device design and integration.

ACKNOWLEDGMENT

This work was supported by the Science and Engineering Research Council of A*STAR (Agency for Science, Technology and Research), Singapore (Grant No. A20G9b0135).

REFERENCES

[1] S. Shao, Z. Luo, and T. Wu, "High figure-of-Lamb wave resonators based on Al0.7Sc0.3N thin film," IEEE Electron Device Lett., vol. 42, pp. 1378–1381, September 2021.

[2] D. K. T. Ng, C. P. Ho, L. Xu, W. Chen, Y. H. Fu, T. Zhang, L. Y. Siow, N. Jaafar, E. J. Ng, Y. Gao, H. Cai, Q. Zhang, and L. Y. T. Lee, "NDIR CO2 gas sensing uaing CMOS compatible MEMS ScAlN-based pyroelectric detector," Sensors Actuators B. Chem., vol. 346, pp. 130437, July 2021.

[3] N. Wang, Y. Zhu, G. L. Chua, B, Chen, S. Merugu, N. Singh, and Y. Gu, "Over 10% of k_{eff}^2 demonstrated by 2-GHz spurious mode-free $Sc_{0.12}Al_{0.88}N$ laterally coupled alternating thickness mode resonators," IEEE Electron Device Lett., vol. 40, pp. 957-960, June 2019.

[4] T. Aubert, J. Bardong, O. Legrani, O. Elmazria, M. B. Assouar, G. Bruckner, and A. Talbi, "In situ high-temperature characterization of AlN-based surface acoustic waver devices," J. Appl. Lett., vol. 114, pp. 014505, July 2013.

[5] R.Farrell, V. R. Pagan, A. Kabulski, S. Kuchibhatla, J. Harman, K. R. Kasarla, L. E. Rodak, P. Famouri, J. P. Hensel, and D. Korakakis, "High temperature rannealing studies on the piezoelectric properties of thin aluminum nitride films," MRS Online Proc. Library, vol. 1052, pp. 618-623, May 2008.

[6] P. Musavigharavi, A. C. Meng, D. Wang, J. Zhang, A. C. Foucher, R. H. Olsson III, and E. A. Stach, "Nanoscale structural and chemical properties of ferroelectric aluminum scandium nitride thin films,", J. Phys. Chem. C, vol. 125, pp. 14394-14400, June 2021.

[7] X. Liu, J. Zheng, D. Wang, P. Musavigharavi, E. A. Stach, R. Olsson III, and D. Jariwala, "Aluminum scandium nitride-based metal-ferroelectric-metal dioda memory devices with high on/off ratios," Appl. Phys. Lett., vol. 118, pp. 202901, May 2021.

[8] D. Wang, J. Zheng, P. Musavigharavi, W. Zhu, A. C. Foucher, S. E. Trolier-McKinstry, E. A. Stach, and R. H. Olsson III, "Ferroelectric switching in sub-20 nm aluminum scandium nitride thin films," IEEE Electron Device Lett., vol. 41, pp. 1774-1777, December 2020.

[9] M. Li, B. Chen, J. Xie, W. Song, and Y. Zhu, "Effects of post-annealinh on texture evolution of sputtered ScAlN films," IEEE Int, Ultrasonic Symp. (IUS), September 2020.

[10] M. Li, K. Hu, H. Lin, and Y. Zhu, "Structural characterization of the abnormal grains evolution in sputtered ScAlN films," IEEE Int, Ultrasonic Symp. (IUS), September 2021.

[11] R. E. Galindo, R. Gago, D. Duday, and C. Palacio, "Towards nonametric resolution in multilayer depth profiling: a comparative study of RBS, SIMS, XPS and GDOES," Anal. Bioanal. Chem., vol. 396, pp. 2725-2740, January 2010.

[12] R. Korbutowicz, A. Zakrzewski, O. Rac-Rumijowska, A. Stafiniak, and A. Vincze, "Oxidation rates of aluminium nitride thin films: effect of composition of the atmosphere," J. Mater. Sci.: Mater Electron, vol. 28, pp. 13937-13949, June 2017.

[13] Z. Fang, E. Wang, Y. Chen, X. Hou, K. Chou, W. Yang, J. Chen, and M. Shang, "Wurtzite AlN(0001) surface oxidation: hints from ab initio calculations," ACS Appl. Mater. Interfaces, vol. 10, pp. 30811-30818, August 2018.

[14] M. A. Signore, E. Bellini, A. Taurino, M. Catalano, M. C. Martucci, P. Creti, L. Vasanelli, P. Siciliano, and F. Quaranta, "Structural and morphological evolution of aluminum nitride thin films: influence of additional energy to the sputtering process," J. Phys. Chem. Solids, vol. 74, pp. 1444-1451, May, 2013.

[15] H. Cheng, Y. Sun, and P. Hing, "The influence of deposition conditions on structure and morphology of aluminum nitride films deposited by radio frequency reactive sputtering," Thin Solid Films, vol. 434, pp. 112-120, February 2003.

[16] M. Yamashita, Y. Sasaki, H. Ito, H. Ohsata, and N. Shabata, "Fabrication of aluminum nitride film and its oxidation behavior," J. Soc. Mater. Sci. Japan, vol. 55, pp. 785-789, August 2006.